Scientia Iranica B (2015) 22(1), 175–186

Sharif University of Technology
Scientia Iranica
Transactions B: Mechanical Engineering
www.scientiairanica.com

Simulation of flow over a confined square cylinder and optimal passive control of vortex shedding using a detached splitter plate

P. Ghadimi*, S.R. Djeddi, M.H. Oloumiyazdi and A. Dashtimanesh[1]

Department of Marine Technology, Amirkabir University of Technology, Tehran, P.O. Box 15875-4413, Iran.

Received 26 August 2012; received in revised form 15 April 2014; accepted 6 October 2014

KEYWORDS
Confined square cylinder;
Splitter plate;
Finite difference method;
Vortex shedding;
Vorticity-stream function;
Optimal passive control.

Abstract. In the area of bluff body aerodynamics, controlling the vortex shedding is of great importance to prevent damages caused by the vortex-induced forces. Accordingly, a short and thin splitter plate has been utilized at different downstream positions to interfere with the vortex wake of a confined square cylinder in the framework of an optimal passive control study. Vorticity-stream function formulation and finite-difference method have been used to numerically simulate the two-dimensional laminar flow. For preventing the flow from becoming three-dimensional, the Reynolds number is kept below 250. Validation of the code and mesh dependency analysis are offered. Based on the flow patterns acquired, the optimal position of the splitter plate behind the cylinder can prevent the detachment of the pair of vortices from the cylinder and will keep the streamlines symmetric around the zero streamline. Consequently, vortex shedding does not occur and the vortex-induced forces are eliminated entirely. Interestingly we showed that the vortex can be suppressed even when the splitter plate is asymmetrically arranged behind the cylinder, especially in the case of positioning the body close to the surrounding walls.

1. Introduction

Fluid flow over bluff bodies has been of great concern in a variety of engineering research for a long time. Aerodynamics of bluff bodies is an important issue in those studies. Separation and vortex shedding are the common phenomena which take place in relatively low Reynolds numbers due to high positive pressure gradient. Vortex shedding causes fluctuation of pressure distribution on the body surface. Due to the vortex-induced forces, the body oscillates with a definite frequency. This may cause serious damages to different structures such as suspended bridges and offshore oil platforms. However, nature takes advantage of these vortices intelligently. For example, boxfish which has a bony blunt body is able to move and maneuver easily even in highly turbulent water streams due to shedding of vortices.

In the current study, incompressible laminar flow over a square cylinder as a bluff body, and the effects of a short and thin splitter plate in tandem have been analyzed. Most researches on bluff bodies have been devoted to fluid flow over circular cylinders and analysis of flow over square cylinders is rare in the literature. Among those considering two-dimensional square cylinder as the bluff body, Okajima et al. [1], Davis et al. [2], Mukhopadhyay et al. [3], Suzuki et al. [4], and Breuer et al. [5] have investigated the flow over a confined square cylinder with different Reynolds numbers and blockage factors. It should be noted that,

1. *Present address: Faculty of Engineering, Persian Gulf University, Bushehr, Iran.*
*. *Corresponding author. Tel.: +98 21 64543117; Fax: +98 21 66412495*
E-mail address: pghadimi@aut.ac.ir (P. Ghadimi)

when the cylinder is confined, two extra parameters have to be taken into account. These parameters are inflow velocity profile and blockage factor which is defined as the ratio of square side length to the channel width. In the following, a brief literature review of the control of vortex shedding from a square cylinder is presented.

Obasaju [6] carried out an experiment to investigate the effect of end plates on pressure distribution on a three-dimensional square section cylinder with a span-to-side ratio of 18:1. He measured mean pressures for Reynolds numbers in the range of 30,000 to 120,000. His results exhibited sensitivity of base pressure in the separated flow region to the type of end plates used. Particularly for high angles of incidence ($\alpha \geq 15°$), small end plates were found to decrease the base suction whereas large end plates were found to increase the base suction and drag. Nakagawa [7] experimentally explored the effects of a small airfoil-shaped splitter plate on the vortex shedding from a single square prism at free-stream Mach numbers between 0.15 and 0.91 and a constant spacing ratio. He found out that, when no shock waves exists in the flow, the Strouhal number is almost independent of the Mach number and takes about 0.11, which is smaller than the value of 0.13, known for a single square prism. However, as soon as shock waves appear in the flow, the Strouhal number increases suddenly and then further increases with increasing of the Mach number. Park and Higuchi [8] simulated the unsteady separated flow around a square cylinder to investigate the wake flow control by a splitter plate attached to the base of the cylinder. Instantaneous flow patterns were scrutinized to see how the splitter plate affects the vortex formation behind the body and the downstream shedding. They concluded that the drag and the frequency were significantly reduced by the splitter plate, suppressing vortex shedding in the wake. Bruneau and Mortazavi [9] investigated the passive control of bluff body (square cylinder) flows using porous media by means of the penalization method. This method is used to create intermediate porous media between solid obstacles and the fluid in order to modify the boundary layer behavior. Their study covered a wide range of two-dimensional flows from low transitional flow to the fully established turbulence by direct numerical simulation of incompressible Navier-Stokes equations. They illustrated the effect of the porous layer permeability and thickness on the passive control. The results revealed the ability of porous media to both regularize the flow and to reduce the drag forces up to 30%. Zhou et al. [10] placed a control plate upstream of a square cylinder. The control plate height was varied from 10% to 100% of the square side width, and for each height, the distance between the control plate and the cylinder was varied from 0.5 to 3.0 times of the square width. The simulation was carried out by considering the Reynolds number to be 250. The results showed a significant reduction in drag and suppression of fluctuating lift on the square cylinder. Doolan [11] in his recent work placed an infinitely thin flat plate downstream of a square cylinder with a length of 0.834 of the cylinder side length along the zero streamline. Furthermore, the distance between the square cylinder and the plate was considered to be 2.37 of the cylinder side length. The flow was simulated with a Reynolds number of 150 and he reported that the force on the square cylinder was reduced significantly. However, the amplitude of the lift coefficient on the downstream plate was found to be the same as that for the single square cylinder.

One of the important issues which must be addressed is the fact that, for flow over square cylinder, in contrast to flow over circular cylinder, the separation points are definite. At Reynolds numbers lower than 100, flow separates at the trailing edge, and at higher Reynolds numbers, separation occurs at the leading edge. Etminan et al. [12] analyzed flow over two equal square cylinders in tandem arrangement in order to study the influence of Reynolds number and the onset of vortex shedding on the flow patterns. The distance between cylinders had been kept constant. They found that the onset of vortex shedding occurs for a Reynolds number varying from 35 to 40. Ali et al. [13] numerically investigated the interaction of a square cylinder wake with a downstream plate at $Re = 150$. They concluded that, if the position of the plate is optimal, considerable reductions in vortex shedding frequency, root mean square of lift and drag of the cylinder occur. Gnatowska [14] studied aerodynamic loads of two prismatic bodies in tandem arrangement. The flow had been considered turbulent. It was found that periodical flow disturbances bring about a rapid growth of surface pressure and wall shear stress fluctuations.

The passive control of flow induced forces which is also the case study of the present paper has been addressed in some works in nearly the past decade. Kwon and Choi [15] have studied the laminar vortex shedding behind a circular cylinder and its control using attached splitter plates downstream. The passive control is achieved through changing the length of the splitter plate, and results stated that the critical length of the plate would be close to that of the cylinder diameter. Anderson and Szewczyk [16] investigated the near wake of a circular cylinder at subcritical Reynolds numbers between 2700 to 46000. Two and three-dimensional configurations of the cylinder and the downstream attached splitter plate were incorporated inside a wind tunnel. Experimental results with different flow characteristics showed that a splitter plate reduced the level of three-dimensionality

in the formation region by stabilizing the transverse 'flapping' of the shear layers. As one of the most comprehensive studies, Ozono [17] studied the flow around a circular/rectangular cylinder behind which a short thin splitter plate was inserted horizontally as an interference element. This plate is moved streamwise and spanwise in order to achieve an optimal position. The mainly used Reynolds number was 17000 and all experimental results showed the increase in Strouhal number due to vortex suppression. In more recent works, Mahbub Alam et al. [18] addressed the suppression of fluid force acting on two square prisms in a tandem arrangement in which a flow approaching the upstream prism was controlled by a thin flat plate. The position of the control plate upstream and also the position of the downstream prism were varied in order to achieve an optimal position and a significant decrease in fluid forces acting on both prisms was observed for a certain range of control plate positions. In a similar approach, Zhang et al. [19] examined the aerodynamic characteristics of a square cylinder with an upstream rod in a staggered arrangement. The pressure measurement was conducted in a wind tunnel at a Reynolds number of 82000 and the flow visualization was carried out in a water tunnel at a Reynolds number of 5200. The passive flow control method using different positions and staggered angles of the upstream rod leads to the reduction of the drag coefficient of the square cylinder. In this framework of upstream positioning of the control plates, Mahbub Alam et al. [20] investigated the effect of a T-shaped plate on reduction of fluid forces on two tandem circular cylinders in a uniform cross-flow at a Reynolds number of 65000. The T-shaped plate is used as the control object and is placed upstream of the cylinder in order to control the approaching flow. Experimental results of the wind tunnel test section prove that the optimum reduction in fluid forces occurs with an optimal trail length of the T-shape plate carefully positioned upstream. Finally, in one of the most recent works in this field, Ali et al. [21] studied the effects of an attached splitter plate on the passive control of the fluid flow induced forces acting on a square cylinder. The numerical study was carried out at a Reynolds number of 150 and the length of the attached splitter plate was varied systematically in order to achieve the optimal configuration. The effect of the plate on suppressing the fluctuating lift forces is shown through the numerical results.

In the present study, the effects of a short and thin splitter plate on vortex shedding from a square cylinder in an incompressible laminar flow has been investigated. Flow patterns in an instant of time and the time history of the Lift force acting on the cylinder have been examined to explore the effect of the splitter plate on vortex formation downstream of the cylinder. Previously, Chan and Jameson [22] utilized this method to suppress vortex-induced forces on a circular cylinder. However, application of this method to two-dimensional square cylinders conducted by the current authors is a new attempt to control the vortex shedding phenomenon. Here, the position of the cylinder inside the channel has been changed and the ground effects have been analyzed. The splitter plate is also moved vertically and horizontally in order to obtain the optimum position which will have the best effect on suppressing the lift force oscillations through an extensive optimal passive control problem which will be addressed in Section 4.2. Therefore, the detachment of the downstream plate, streamwise and spanwise positioning of the control object at low Reynolds number flow and extensive numerical and parametric studies distinguish the present work from the previous efforts in this field.

2. Governing equations

The fluid in the current investigation is considered to be incompressible, viscous, and Newtonian. Due to the fact that temperature is constant throughout the flow field, density and viscosity of the fluid remain constant as well. As a result, energy equation can be decoupled from the governing equations and the incompressible Navier-Stokes equations as well as the continuity equation have to be solved simultaneously. These equations in two-dimensional form are:

$$\frac{\partial u}{\partial x}+\frac{\partial v}{\partial y}=0, \tag{1}$$

$$\frac{\partial u}{\partial t}+u\frac{\partial u}{\partial x}+v\frac{\partial u}{\partial y}=-\frac{1}{\rho}\frac{\partial p}{\partial x}+\vartheta\left(\frac{\partial^2 u}{\partial x^2}+\frac{\partial^2 u}{\partial y^2}\right), \tag{2}$$

$$\frac{\partial v}{\partial t}+u\frac{\partial v}{\partial x}+v\frac{\partial v}{\partial y}=-\frac{1}{\rho}\frac{\partial p}{\partial y}+\vartheta\left(\frac{\partial^2 v}{\partial x^2}+\frac{\partial^2 v}{\partial y^2}\right), \tag{3}$$

where u and v are velocity components in x and y directions, respectively; p is pressure; ρ is density; and ϑ is the kinematic viscosity of the fluid.

It should be noted that the body forces have been neglected for simplicity. Moreover, due to vortex shedding, the flow is unstable and the terms containing time derivatives cannot be neglected. In this study, pressure distribution in the flow field is not of great concern. Pressure is eliminated from Eqs. (2) and (3) by cross-differentiation. Thus, we obtain:

$$\frac{\partial \omega}{\partial t}+u\frac{\partial \omega}{\partial x}+v\frac{\partial \omega}{\partial y}=\vartheta\left(\frac{\partial^2 \omega}{\partial x^2}+\frac{\partial^2 \omega}{\partial y^2}\right), \tag{4}$$

where ω is vorticity in the z direction. Considering the definition of stream function, ψ, and vorticity are:

$$u = +\frac{\partial \psi}{\partial y}, \tag{5}$$

$$v = -\frac{\partial \psi}{\partial x}, \tag{6}$$

$$\omega = \frac{\partial v}{\partial x} - \frac{\partial u}{\partial y}. \tag{7}$$

The governing equations can be declared in the following form, i.e. the vorticity transport equation and a Poisson's equation relating vorticity to stream function:

$$\frac{\partial \omega}{\partial t} + \frac{\partial \psi}{\partial y}\frac{\partial \omega}{\partial x} - \frac{\partial \psi}{\partial x}\frac{\partial \omega}{\partial y} = \vartheta\left(\frac{\partial^2 \omega}{\partial x^2} + \frac{\partial^2 \omega}{\partial y^2}\right), \tag{8}$$

$$\frac{\partial^2 \psi}{\partial x^2} + \frac{\partial^2 \psi}{\partial y^2} = -\omega. \tag{9}$$

Eq. (8) is actually the famous Helmholtz equation of hydrodynamics which has been simplified by elimination of the vortex-stretching term due to the fact that vortex-stretching is a three-dimensional phenomenon and this term vanishes in the two-dimensional flows [23].

3. Discretization of equations

Finite-difference method has been utilized for discretization of governing equations. Accuracy of discretizations is first order in time and second order in space. Moreover, forward difference quotient has been used for time derivative while central difference quotient has been applied for space derivatives. The algebraic equations which approximate the governing partial differential equations are as follows:

$$\begin{aligned}\frac{\omega_{i,j}^{n+1} - \omega_{i,j}^{n}}{\Delta t} &+ \frac{\psi_{i,j+1}^{n} - \psi_{i,j-1}^{n}}{2\Delta y}.\frac{\omega_{i+1,j}^{n} - \omega_{i-1,j}^{n}}{2\Delta x} \\ &- \frac{\psi_{i+1,j}^{n} - \psi_{i-1,j}^{n}}{2\Delta x}.\frac{\omega_{i,j+1}^{n} - \omega_{i,j-1}^{n}}{2\Delta y} \\ &= \vartheta\left(\frac{\omega_{i+1,j}^{n} - 2\omega_{i,j}^{n} + \omega_{i-1,j}^{n}}{(\Delta x)^2}\right. \\ &\left. + \frac{\omega_{i,j+1}^{n} - 2\omega_{i,j}^{n} + \omega_{i,j-1}^{n}}{(\Delta y)^2}\right).\end{aligned} \tag{10}$$

$$\begin{aligned}\frac{\psi_{i+1,j}^{n} - 2\psi_{i,j}^{n} + \psi_{i-1,j}^{n}}{(\Delta x)^2} &+ \frac{\psi_{i,j+1}^{n} - 2\psi_{i,j}^{n} + \psi_{i,j-1}^{n}}{(\Delta y)^2} \\ &= -\omega_{i,j}^{n}.\end{aligned} \tag{11}$$

3.1. Boundary conditions

To solve the discretized equations, no-slip boundary condition has been imposed on all solid walls. Furthermore, stream function on each solid wall is a constant value. At the inflow section, a parabolic velocity profile has been prescribed. Since the component of velocity in the y direction is zero at the inflow section, stream function is a function of y only and its profile can be obtained using Eq. (5), where H is the channel height:

$$\psi_{1,j} = u_{\max}\left(y_j - \frac{4y_j^3}{3H^2}\right). \tag{12}$$

At the outflow section, the y-component of the velocity has been taken to be zero. Based on Eq. (6), derivative of stream function in x direction must be zero, too. Accordingly, the following relation would be derived for the stream function at the outflow section:

$$\psi_{N,j} = \frac{1}{3}(4\psi_{N-1,j} - \psi_{N-2,j}). \tag{13}$$

Vorticity boundary condition on each solid wall is acquired by Taylor expansion of stream function [24]. For example, the vorticity boundary condition on the channel lower wall is:

$$\omega_{i,1} = \frac{2}{(\Delta y)^2}(\psi_{i,1} - \psi_{i,2}). \tag{14}$$

At the inflow section, using Eq. (9) and a relation similar to Eq. (14), the vorticity boundary condition would be:

$$\omega_{1,j} = \frac{2}{(\Delta x)^2}(\psi_{1,j} - \psi_{2,j}) - \frac{\psi_{1,j+1} - 2\psi_{1,j} + \psi_{1,j-1}}{(\Delta y)^2}. \tag{15}$$

For the outflow section, a similar boundary condition can be obtained. The boundary conditions as discussed above are shown in Figure 5.

3.2. Pressure computation

In order to obtain the pressure distribution inside the computational domain, the well-known Poisson's equation of pressure must be implemented:

$$\begin{aligned}\frac{\partial^2 P}{\partial x^2} + \frac{\partial^2 P}{\partial y^2} &= -\left(\frac{\partial u}{\partial x}\right)^2 + \left(\frac{\partial v}{\partial y}\right)^2 \\ &\quad - 2\left(\frac{\partial u}{\partial y}\right)\left(\frac{\partial v}{\partial x}\right),\end{aligned} \tag{16}$$

where P is the pressure. The pressure equation is solved using Successive-Over-Relaxation (SOR) iterative method and the relaxation factor is set to be 1.6 for the improved convergence behavior. By integrating the pressure over the cell faces (lines in 2D case), the pressure-induced lift and drag forces can be evaluated on body.

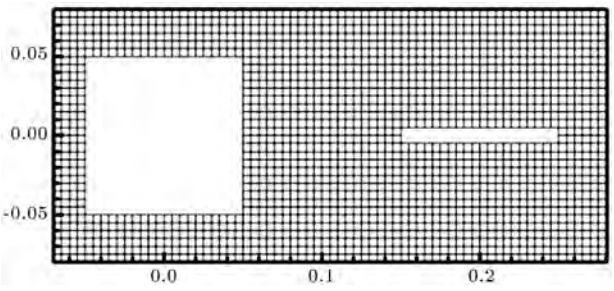

Figure 1. Portion of the generated mesh.

3.3. Computational domain and generated mesh

The computational domain has been extended 10 times the square side length at the upstream and 20 times of this value at the downstream of the cylinder. The length and thickness of the splitter plate are considered to be equal to that of the square side length and 0.1 of the square side length, respectively. Grid points in the domain have been distributed uniformly as $\Delta x = \Delta y = 0.005$ based on a mesh convergence study addressed in Section 4.1. Also, a time step size of $\Delta t = 0.002$ (s) is maintained in order to keep the maximum Courant number below unity for stability reasons. Moreover, all the instantaneous results are shown at the time $t = 190$ (s). It is known that at this instant of time, the flow is fully developed and vortices have been distributed all over the downstream of the flow. In Figure 1, a portion of the generated mesh has been presented.

4. Results and discussion

As discussed earlier, in order to keep the two-dimensionality of the flow patterns and vortices, the Reynolds number should be kept below 250. As a result of this and in order to broaden the extents of this study, flow simulations have been carried out for two different cases, i.e. for Reynolds numbers of 100 and 200. In each case, the distance between the square cylinder and the splitter plate has been varied vertically and horizontally in order to find the optimal position for the splitter plate in the framework of an optimal passive control problem discussed in Section 4.2.

4.1. Validation of the numerical code

In the absence of any existing data regarding the case with a splitter, an attempt is made to validate the results for the case without a splitter for which there is an existing data available. Once the validation verifies the accuracy of the code, parametric studies will be performed to examine different effects of the splitter on the vortex shedding.

The developed CFD code has been validated by comparing the recirculation lengths obtained by the developed code at relatively low Reynolds numbers ($10 \leq \mathrm{Re} \leq 50$), to those obtained by Breuer et al. [5].

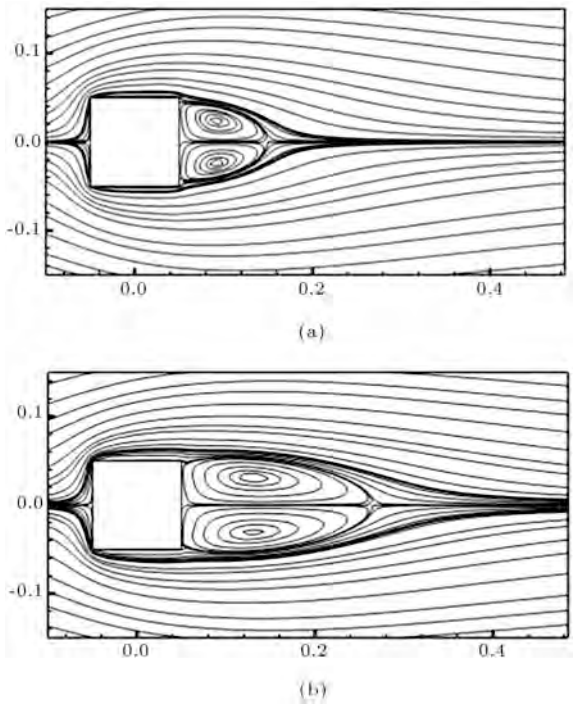

Figure 2. Streamlines in flow over the confined square cylinder with $\beta = 1/8$: (a) $\mathrm{Re} = 20$; and (b) $\mathrm{Re} = 40$.

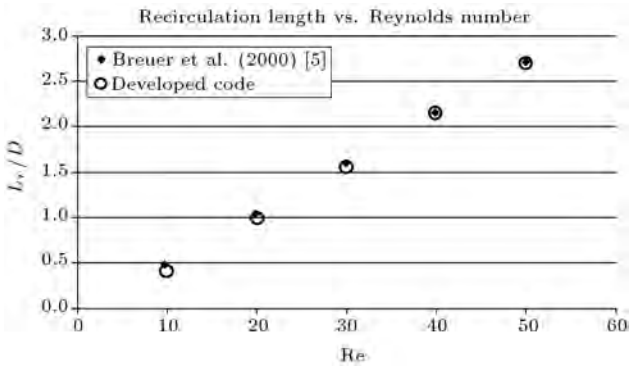

Figure 3. Recirculation length versus Reynolds number for $\beta = 1/8$.

It should be noted that the Reynolds number is based on the maximum inlet velocity and the square side length, just the same as what is done by Breuer et al. Furthermore, all of the results presented are at the time instant of 5.0 seconds.

Figure 2 shows the streamlines in flow over the confined square cylinder with the blockage factor of 1/8 and Reynolds numbers of 20 and 40.

Comparison between the obtained recirculation length and that obtained by Breuer et al. [5] is illustrated in Figure 3 which shows good agreement.

As discussed above, in order to evaluate the efficiency of the splitter plate, the lift forces acting on the cylinder should be measured and compared with the case without the splitter plate. Based on this approach, one can find out where the splitter plate

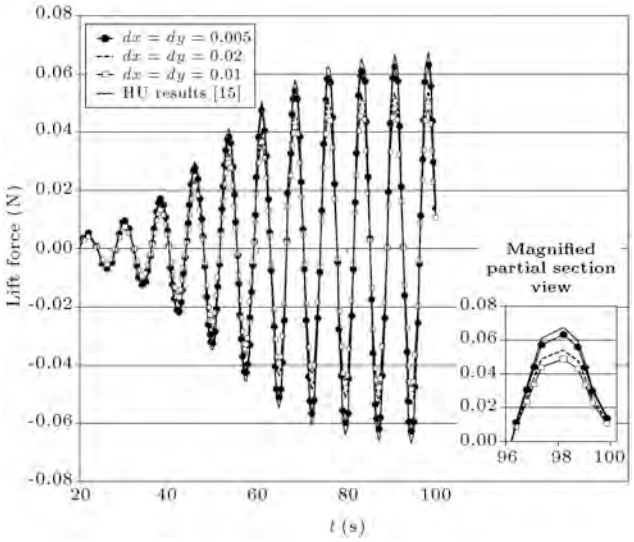

Figure 4. Evaluated lift force on the cylinder using different grid sizes in comparison with previous numerical results [25].

should be placed to obtain minimum lift amplitude acting on the cylinder. Also, the dependency of the results on the grid size should be studied which leaves us with a mesh convergence analysis. The pressure lift force acting on the body will then be compared to some numerical results in the literature [25] using different grid size. Consequently, the validity of the lift force evaluation and the mesh convergence will be achieved.

A rectangular section with length and height of 1 m is placed 5 m downstream of the inlet boundary with an inlet velocity of 1 m/s. Reynolds number is preserved at 100 while the flow is determined around the rectangular cylinder. The lift force time history is shown in Figure 4 and a comparison is made between the results in the literature and the results obtained by the current numerical code on different grid sizes.

Results show that, with the increase of mesh quality, the evaluated lift force will get closer to the numerical results of Hu [25] and the results agreed well using $\Delta x = \Delta y = 0.005$. The Strouhal number of $\mathrm{St} = \frac{fD}{U} = 0.138$ is calculated for the case of $\mathrm{Re} = 100$ which agrees well with the benchmark solutions of [5]. Similar results were achieved at a Reynolds number of 200 with nearly the same Strouhal number, i.e. $\mathrm{St} = 0.139$. In addition to the standard grid convergence study, the rms magnitudes of the lift coefficient for different levels of grid refinement with refinement ratio of 2 were checked based on the Grid Convergence Index (GCI) criterion [26]. The ratio of 0.997118 (nearly 1.0) shows that the solution is in the asymptotic range and the GCI of 1.66% proves that the grid resolution is fine enough for the solution to be independent of the mesh sizes. The obtained results for the grid convergence study based on GCI are in good agreement with the study and investigations of Ali et al. [27] on this particular issue. Therefore, the mesh dependency has been satisfied and the grid size of $\Delta x = \Delta y = 0.005$ will be used for other cases as mentioned in Section 3.3.

4.2. Optimal passive control problem

As previously stated in Section 4, flow around the rectangular cylinder is analyzed for two different Reynolds numbers of 100 and 200. Contrary to the flow around circular cylinder in which Reynolds number of 180 or 161 is introduced as the starting point for the formation of 3D structures in the wake, there has not been an accurate and comprehensive study on this phenomenon for flow around rectangular cylinders. As a hint, Reynolds number of 300 has been introduced by Franke [28] as starting point of this phenomenon. Breuer et al. [5] stated that this criterion is slightly beyond the limit of 2D simulation and the disturbances which occur in the periodic nature of 2D vortex shedding has proved this theory. They studied flow around rectangular cylinder for the blockage coefficient of 1/8 by two different methods of Finite Volume Method (FVM) and Lattice-Boltzmann Method (LBM). The experimental studies of Dutta et al. [29] have verified the results of Breuer et al. [5] and showed that beyond the Reynolds number of 200, aspect ratio of cylinder has to be taken into account due to the formation of 3D structures.

In the present study, the final Reynolds number at which the flow has been simulated is set to be $\mathrm{Re} = 200$. The reason for this limit can be sought in the change of principal behaviors in the flow pattern with further increase of the Reynolds number from this particular limit. The frequency of vortex shedding will rise and therefore the laminar shedding will no longer remain 2-dimensional. Further studies in 3-dimensional case have proved this statement that the flow at Reynolds numbers above 200 will experience 3-dimensional instabilities and vortices. Also, in 2-D simulations, deviations from fully periodic structures have been recorded which restate the above theory. It should also be noted that Reynolds number based on the height of the inlet boundary has already reached the value of $\mathrm{Re} = 1000$ and therefore further increase of Reynolds number would need special treatment for the turbulence flow parameters.

Also, the rectangular cylinder is moved closer to the channel walls at two different positions addressed by a k factor defined as:

$$k = \frac{L_w}{D}. \tag{17}$$

Dimensions of the computational domain and the position of the rectangular cylinder and the splitter plate can be seen in Figure 5.

Each case (i.e. combinations of two Reynolds numbers and 3 rectangular cylinder vertical positions)

Table 1. RMS magnitudes of lift force measured for all different cases.

Re	k	No splitter	$L = 1D$			$L = 2D$			$L = 3D$			$L = 4D$
			$H1$	$H2$	$H3$	$H1$	$H2$	$H3$	$H1$	$H2$	$H3$	$H1$
100	1.5	**0.147543**	8.49E-06	-	-	**1.41E-06**	-	-	0.193109	-	-	0.221959
	1.0	**0.105846**	2.83E-06	2.83E-06	2.12E-06	2.12E-06	1.41E-06	**7.07E-07**	0.132298	0.135127	0.13746	-
	0.5	**1.99E-06**	3.54E-06	2.12E-06	3.54E-06	2.83E-06	1.41E-06	1.41E-06	1.41E-06	**7.07E-07**	2.83E-06	-
200	1.5	**0.317134**	0.095034	-	-	**1.41E-06**	-	-	0.301649	-	-	0.330852
	1.0	**0.278315**	0.065972	0.072973	0.067104	1.41E-06	**7.07E-07**	0.036628	0.270749	0.271668	0.275415	-
	0.5	**0.054871**	0.016051	2.83E-06	2.83E-06	0.008132	2.83E-06	**2.12E-06**	0.009334	0.002546	0.00396	-

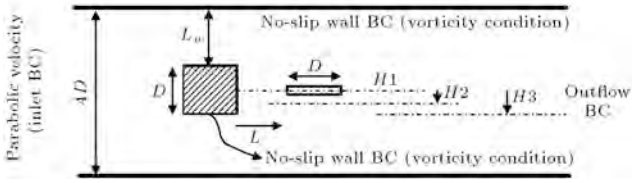

Figure 5. Rectangular cylinder along with splitter plate inside the computational domain in their different positions showing the boundary conditions.

is first analyzed without the splitter plate and the lift force amplitude is evaluated. The splitter plate is then added and placed at 6 different vertical and horizontal downstream positions of the cylinder. For all cases of study, rms magnitudes of the lift force are measured based on a selected number of cycles after flow parameters reach periodically steady states; these values are listed in Table 1.

The highlighted cells in the right side of the Table 1 show the best results achieved with the case of the splitter plate. Region $0 < L < 2D$ demonstrates the best horizontal position of the splitter plate streamwise while the case of $L = 4D$ at symmetrical cylinder position (i.e. $k = 1.5$) shows that, for the position of $L > 4D$ the splitter plate would have no effect on the amplitude of the lift force acting on the cylinder. Another conclusion which can be drawn from the above mentioned results is that, in the case of $k = 1.5$ at which the cylinder is in its closest position to the wall, the splitter plate should be placed far from the symmetric line of the cylinder in order to achieve better results.

The Strouhal numbers for the symmetrical case of $k = 1.5$ are plotted and compared in Figure 6 against the numerical results of Ali et al. [13] for the case of vortex shedding attenuation using detached plate placed at $L = 2D$. It has been clearly shown that the same results are achieved for nearly all cases where best cancellation is exhibited for $L = 2D$, but in different vertical positions of the splitter plate, i.e. $H1$ for the symmetric case of $k = 0.15$, and $H2$ and

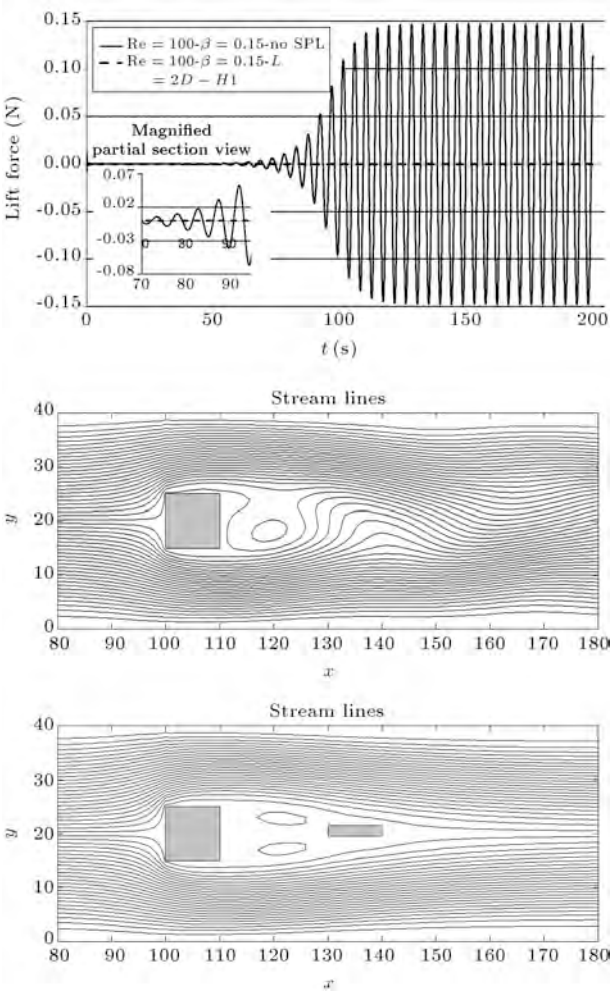

Figure 6. Instantaneous flow patterns and lift force time history in the case of: Re = 100, $k = 1.5$ without splitter (solid curve) and with splitter (dotted curve) in $L = 2D$ and $H1$ position (bottom geometry).

$H3$ for the cases of $k = 0.1, 0.05$ due to the wall effects, respectively. Results of the present numerical method agree well with the benchmark solutions and prove that the effects of the channel walls are low for the symmetric case. This is in contrast with the

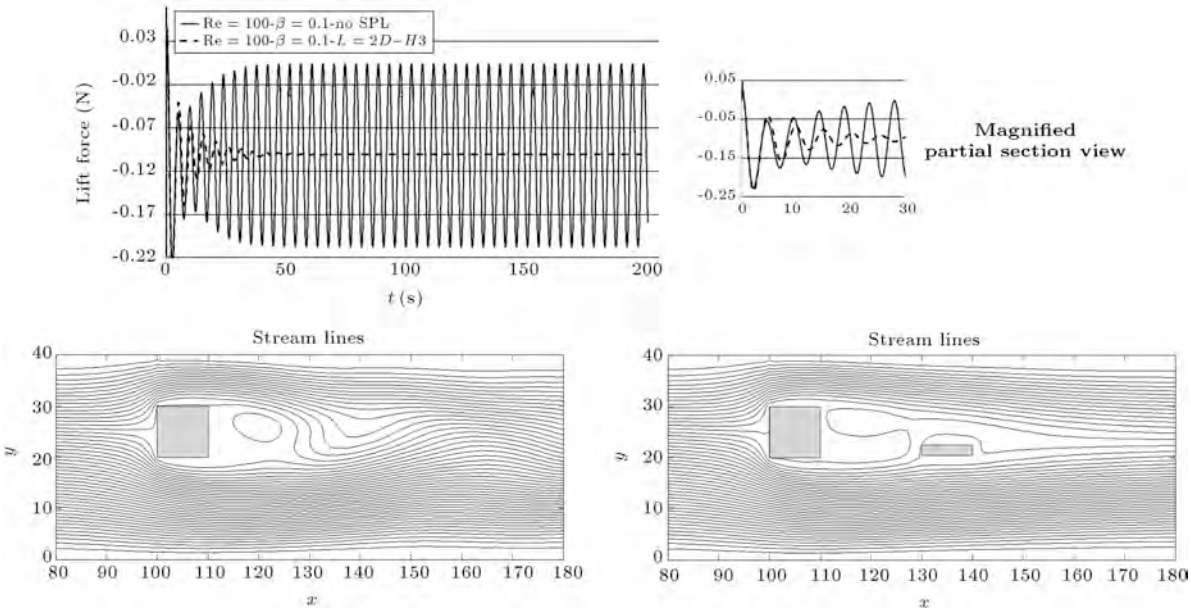

Figure 7. Instantaneous flow patterns and lift force time history in the case of: Re = 100, $k = 1.0$ without splitter (solid curve) and with splitter (dotted curve) in $L = 2D$ and $H3$ position (right geometry).

cases of $k = 0.1$ and $k = 0.05$ with lower Strouhal numbers at both Re = 100 and Re = 200. Also, it has been shown that the lift amplitudes or rms lift force coefficients are majorly attenuated where cancellation is observed while Strouhal numbers will experience minor attenuation even at the optimum position of the splitter plate.

For the case of Re = 100 and $k = 1.0$, the splitter has a significant effect in the range of $0 < L < 2D$ while the best result will be achieved at the cross stream position of $H3$ (far below the symmetric wake line) and more precisely at the streamwise position of $L = 2D$. Results also provide the fact that fluid flow induced fluctuations of the lift force is near zero for the case of $k = 0.5$ (cylinder in its closest position to the wall) at Re = 100. This suggests that in this configuration, the splitter plate is actually not needed but the figures and numbers show that the plate location of $L = 3D$ and $H2$ will lead to the best numerical results in the sense of least lift force amplitude.

For the case of $k = 0.15$, where the rectangular cylinder is placed in the middle of the channel with equal distance from both surrounding walls, the flow is symmetrical and the vertical positions of $H2$ and $H3$ (when the plate is placed below the symmetry line of the rectangular cylinder) are not the case of study, and as shown in Table 1, best cancellation will be achieved for the case of $L = 2D$ and $H1$. A same rationale can be offered for the cases of $k = 0.1$ and $k = 0.05$ as the shedding occurs closer to the cylinder and optimal cancellation are favorably achieved with $L = 2D$ on most cases and $L = 3D$ and $H2$ for $k = 0.05$ at Re = 100.

Instantaneous streamlines and flow patterns for the cases of different Reynolds numbers, and cylinder distance from the wall are shown in Figures 6 through 11, once without the splitter plate and once with the splitter plate at its best position along with the lift force time history on the top. The attenuation of the pressure oscillations are clearly shown in these figures which will result in a less oscillating lift force with much lower amplitude. Due to the large number of simulations that have been performed for the present study and in order to reduce the number of plots, only the instantaneous streamlines showing the flow patterns at a fully developed vortex shedding condition, or later enough after initial cancellation, are shown in these figures. Also as previously stated, in addition to the full time-series and time history diagrams of the lift force, the rms magnitude of the lift for all different cases is given in Table 1.

5. Conclusion

In this study, flow around a rectangular cylinder at low Reynolds numbers is investigated. The rectangular cylinder is confined in a channel with limited width, and the wall effects are taken into account with a parameter, k, which is introduced $k = \frac{L_w}{D}$, and shows how close the rectangular cylinder is placed with respect to the surrounding walls. The flow simulation is studied at two low Reynolds numbers of Re = 100 and Re = 200 where vortex shedding phenomena appear. Laminar flow over a confined square cylinder and a short and thin splitter plate arranged in tandem has been simulated numerically,

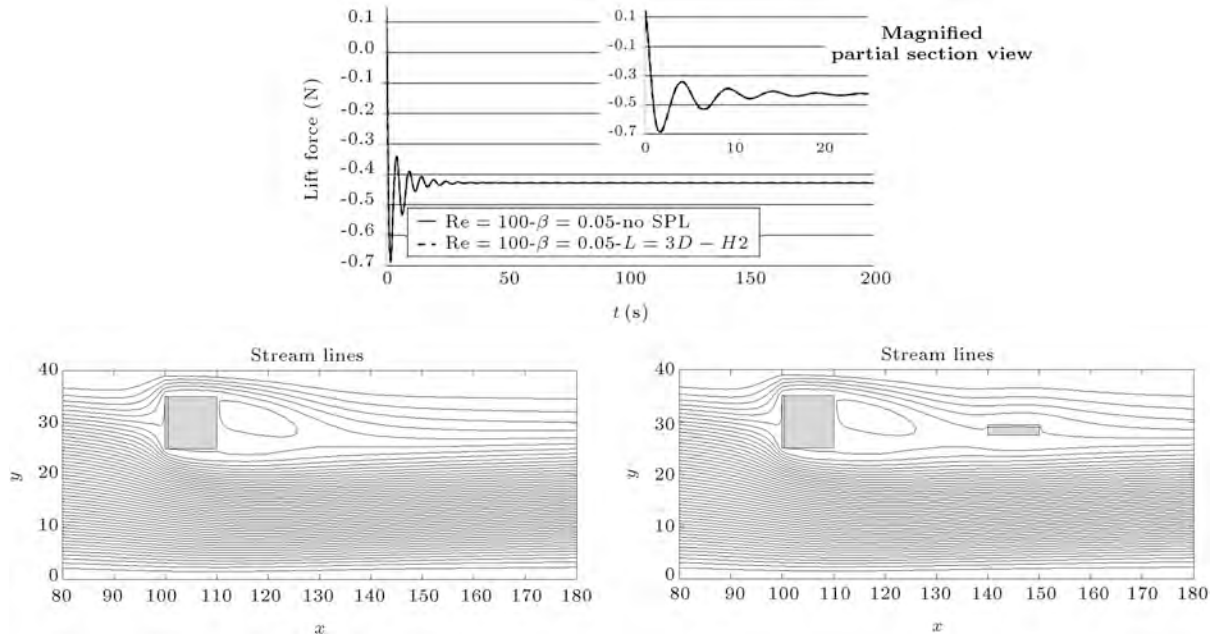

Figure 8. Instantaneous flow patterns and lift force time history in the case of: Re = 100, $k = 0.5$ without splitter (solid curve) and with splitter (dotted curve) in $L = 3D$ and $H2$ position (right geometry).

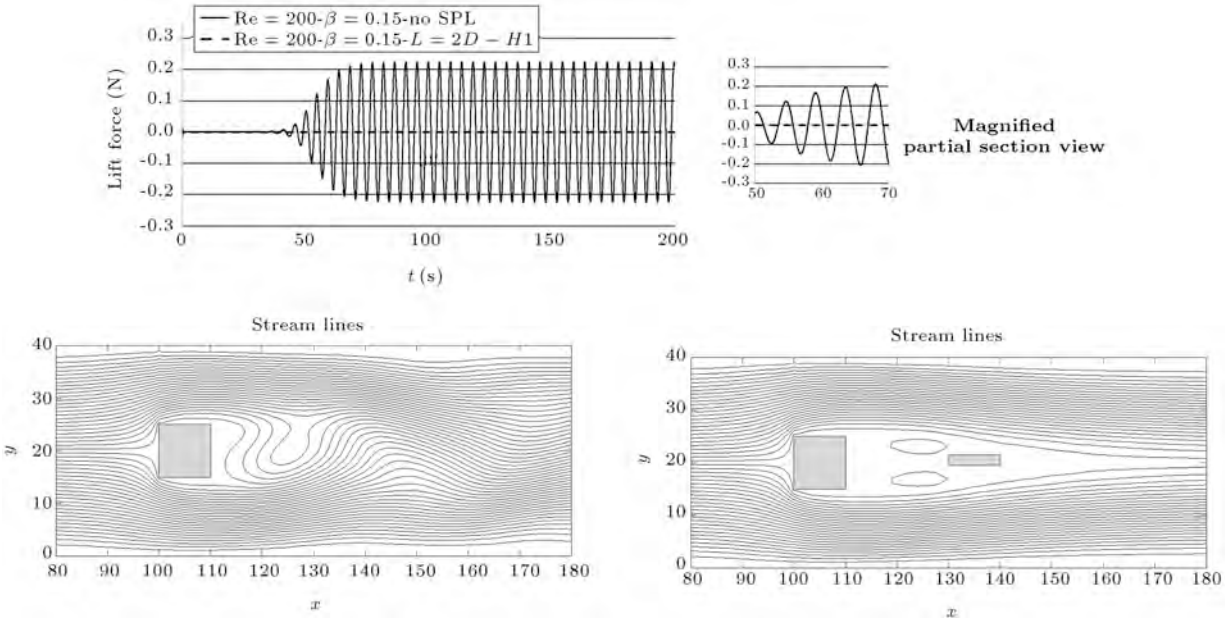

Figure 9. Instantaneous flow patterns and lift force time history in the case of: Re = 200, $k = 1.5$ without splitter (solid curve) and with splitter (dotted curve) in $L = 2D$ and $H1$ position (right geometry).

considering two different Reynolds numbers and three different vertical positions of the cylinder. In this regard, with the aid of a detached splitter plate, the effect of the downstream obstacle on the shedding of vortices is studied.

In each case, the effect and optimal distance of the splitter plate have been investigated using a combination of vertical and horizontal positions of the splitter plate. It has been revealed that according to the flow patterns and the rms magnitude of the lift force amplitude acting on the cylinder, the splitter plate at its best position can attenuate pressure and thus the lift force oscillations which will also lead to much lower lift force amplitudes. Also, in the case of symmetrical flow ($k = 1.5$), when the splitter plate is placed at an appropriate position downstream of the square cylinder, streamlines would become completely symmetrical and the pair of vortices will stay attached

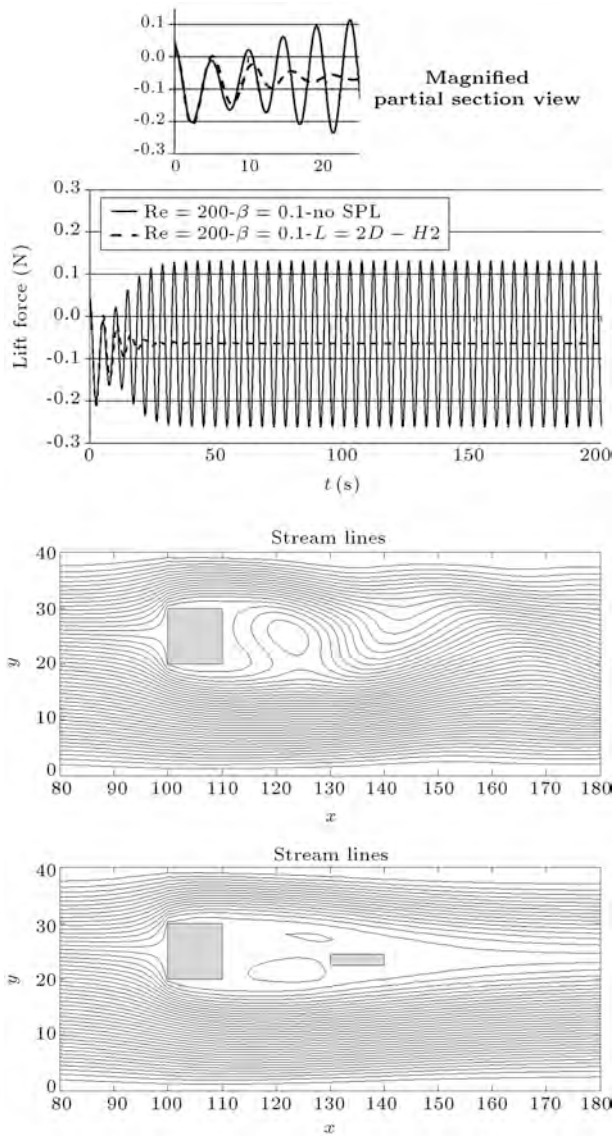

Figure 10. Instantaneous flow patterns and lift force time history in the case of: Re = 200, $k = 1.0$ without splitter (solid curve) and with splitter (dotted curve) in $L = 2D$ and $H2$ position (bottom geometry).

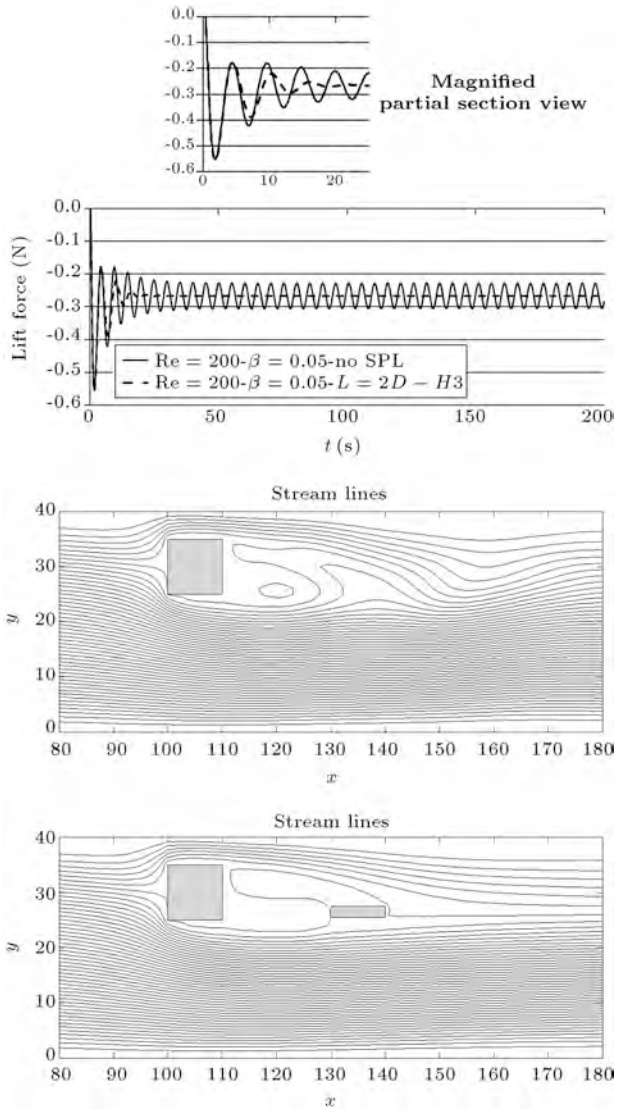

Figure 11. Instantaneous flow patterns and lift force time history in the case of: Re = 200 and $k = 0.5$ without splitter (solid curve) and with splitter (dotted curve) in $L = 2D$ & $H3$ position (bottom geometry).

to the cylinder. As a result, vortex shedding which is the source of fluctuation of the drag and lift forces on the square cylinder can be prevented entirely in some cases using this method. The effect of the channel walls proves to be substantial, especially for the cases of $k = 0.1$ and $k = 0.05$ where the rectangular cylinder is moved closer to the wall. In these conditions, the splitter plate acts more effective, leading to better suppression of the vortex shedding. Due to the large number of cases in the present study and its high computational cost, the blockage factor was set to a constant value which can be changed in future works in order to show the role of this parameter on the effectiveness and the position of the optimum splitter plate. Future works can also be done in the study of different aspect ratios for the splitter plate in order to examine their effects.

Nomenclature

u	x-velocity
v	y-velocity
ω	Vorticity
ψ	Stream function
ν	Kinematic viscosity
H	Channel height
D	Cylinder side length
β	Blockage factor
L	Cylinder to splitter plate distance

k Ratio of side distance of the cylinder from the wall to its width

References

1. Okajima, A., Yi, D., Sakud, A. and Nakano, T. "Numerical study of blockage effects on aerodynamic characteristics of an oscillating rectangular cylinder", *J. Wind Eng. Ind. Aero.*, **67**, pp. 91-102 (1997).
2. Davis, R.W., Moore, E.F. and Purtell, L,P. "A numerical-experimental study of confined flow around rectangular cylinders", *Phys. Fluids*, **27**(1), pp. 46-59 (1984).
3. Mukhopadhyay, A., Biswas, G. and Sundararajan, T. "Numerical investigation of confined wakes behind a square cylinder in a channel", *Int. J. Numer. Meth. Fluids*, **14**, pp. 1473-1484 (1992).
4. Suzuki, H., Inoue, Y., Nishimura, T., Fukutani, F. and Suzuki, K. "Unsteady flow in a channel obstructed by a square cylinder rod (crisscross motion of vortex)", *Int. J. Heat Fluid Flow*, **14**, pp. 2-9 (1993).
5. Breuer, M., Bernsdorf, J., Zeiser, T. and Durst, F. "Accurate computations of the laminar flow past a square cylinder based on two different methods: Lattice-Boltzmann and finite-volume", *Int. J. Heat Fluid Flow*, **21**, pp. 186-196 (2000).
6. Obasaju, E.D. "On the effects of end plates on the mean forces on square sectioned cylinders", *J. Wind Eng. Ind. Aero.*, **5**, pp. 179-186 (1979).
7. Nakagawa, T. "Effects of a small airfoil-shaped splitter plate on vortex shedding from a square prism at subsonic Mach numbers", *Acta Mechanica*, **91**, pp. 11-25 (1992).
8. Park, W.C. and Higuchi, H. "Numerical investigation of wake flow control by a splitter plate", *KSME Int. J.*, **12**(1), pp. 123-131 (1998).
9. Bruneau, C.H. and Mortazavi, I. "Passive control of the flow around a square cylinder using porous media", *Int. J. Numer. Meth. Fluids*, **46**, pp. 415-433 (2004).
10. Zhou, L., Cheng, M. and Hung, K.C. "Suppression of fluid force on a square cylinder by flow control", *J. Fluids Struct.*, **21**, pp. 151-167 (2005).
11. Doolan, C.J. "Flat-plate interaction with the near wake of a square cylinder", *AIAA J.*, **47**(2), pp. 475-479 (2009).
12. Etminan, A., Moosavi, M. and Ghaedsharafi, N. "Determination of flow configurations and fluid forces acting on two tandem square cylinders in cross-flow and its wake patterns", *Int. J. of Mech.*, **2**(5), pp. 63-74 (2011).
13. Ali, M.S.M., Doolan, C.J. and Wheatley, V. "Flow around a square cylinder with a detached downstream flat plate at a low Reynolds number", *17th Australian Fluid Mechanics Conf.* (2010).
14. Gnatowska, R. "Aerodynamic characteristics of two-dimensional sharp-edged objects in tandem arrangement", *Arch. Mech.*, **60**(6), pp. 475-490 (2008).
15. Kiyoung, K. and Haecheon, C. "Control of laminar vortex shedding behind a circular cylinder using splitter plates", *Phys. Fluids.*, **8**(2), pp. 479-486 (1996).
16. Anderson, E.A. and Szewczyk, A.A. "Effects of a splitter plate on the near wake of a circular cylinder in 2 and 3-dimensional flow configurations", *Experiments in Fluids*, **23**, pp. 161-174 (1997).
17. Ozono, S. "Flow control of vortex shedding by a short splitter plate asymmetrically arranged downstream of a cylinder", *Phys. Fluids*, **11**, pp. 2928-2934 (1999).
18. Mahbub Alam, M.D., Moriya, M., Takai, K. and Sakamoto, H. "Suppression of fluid forces acting on two square prisms in a tandem arrangement by passive control of flow", *Journal of Fluids and Structures*, **16**(8), pp. 1073-1092 (2002).
19. Zhang, P.F., Wang, J.J., Lu, S.F. and Mi, J. "Aerodynamic characteristics of a square cylinder with a rod in a staggered arrangement", *Experiments in Fluids*, **38**, pp. 494-502 (2005).
20. Mahbub Alam, M.D., Sakamoto, H. and Zhou, Y. "Effect of a t-shaped plate on reduction in fluid forces on two tandem cylinders in a cross-flow", *J. Wind Eng. Ind. Aerodyn.*, **94**, pp. 525-551 (2006).
21. Ali, M.S.M., Doolan, C.J. and Wheatley, V. "Low Reynolds number flow over a square cylinder with a splitter plate", *Phys. Fluids*, **23**, pp. 033602-1-033602-12 (2011).
22. Chan, A.S. and Jameson, A. "Suppression of vortex-induced forces on a two-dimensional circular cylinder by a short and thin splitter plate interference", Report ACL 2007-5, Aerospace Computing Laboratory, Stanford University (2007).
23. White, F.M., *Viscous Fluid Flow*, 3rd Ed. McGraw-Hill, Singapore (2006).
24. Hoffman, K.A. and Chiang, S.T., *Computational Fluid Dynamics*, 4th Ed., EES, USA (2000).
25. Hu, C. "An Introduction to CFD", *Research Institute for Applied Mechanics*, Kyushu University, Japan (2000).
26. Roache, P.J. "Perspective: A method for uniform reporting of grid refinement studies", *Journal of Fluids Engineering*, **116**(3), pp. 405-41 (1994).
27. Ali, M.S.M., Doolan, C.J. and Wheatley, V. "Grid convergence study for a two-dimensional simulation of flow around a square cylinder at a low Reynolds number", *Seventh Int. Conf. on CFD in the Minerals and Process Ind. CSIRO*, Melbourne, Australia (2009).

28. Franke, R. " Numerical calculation of the unsteady vortex shedding behind cylindrical bodies" [Numerische Berechnung der instationnaren Wirbelablosung hinter zylindrischen Korpern], PhD Thesis. University of Karlsruhe (1991).

29. Dutta, S.H., Panigrahi, P.K. and Muralidhar K. "Experimental investigation of flow past a square cylinder at an angle of incidence", *ASCE J. Engineering Mechanics.*, **134**(9), pp. 788-803 (2008).

Biographies

Parviz Ghadimi received his PhD in Mechanical Engineering in 1994 from Duke University, USA. He served one year as a Research Assistant Professor in M.E. and six years as a Visiting Assistant Professor in Mathematics Department at Duke. He is currently an Associate Professor of Hydromechanics in Department of Marine Technology at Amirkabir University of Technology, Iran. His main research interests include hydrodynamics, hydroacoustics, thermo-hydrodynamics, and CFD. He has authored several scientific papers in these fields.

Seyed Reza Djeddi finished his Bachelor of Science degree in Marine Structures Engineering in Amirkabir University of Technology, in 2006. He was then admitted to the Master of Science degree program in Ship Hydrodynamics at Sharif University of Technology where he successfully defended his MSc thesis in 2009. He is currently a PhD student at the University of Tennessee.

Mohammad H. Oloumiyazdi finished his Bachelor of Science degree in Marine Engineering in Amirkabir University of Technology, in 2011. He was then admitted to the Master of Science degree program in Ship Hydrodynamics at Sharif University of Technology. Mr. Oloumiyazdi is currently working on his MSc thesis.

Abbas Dashtimanesh finished his Bachelor of Science degree in Marine Engineering at the Persian Gulf University. Subsequently, he earned his Master of Science degree in Ship Hydrodynamics from Amirkabir University, in 2008. He was then admitted to the PhD program at the Department of Marine Technology in Amirkabir University of Technology, in 2009. Dr. Dashtimanesh finished his PhD dissertation under supervision of Dr. Ghadimi, in 2013, and as a result of their collaborations, several scientific papers were published in different areas of hydrodynamics. Dr. Dashtimanesh is currently a member of faculty at Persian Gulf University.